Detecting the 1990 Rudbar earthquake-induced landslides, using remote-sensing techniques

Aflaki, M. [1], Ajorlou, N. [2], Ghods, A. [3], Mousavi, Z. [1], Hollingsworth, J. [4]

[1] *Assistant professor, Department of Earth Sciences, Institute for Advanced Studies in Basic Sciences, Zanjan, Iran, aflaki@iasbs.ac.ir, z.mousavi@iasbs.ac.ir*

[2] *PhD student, Department of Earth Sciences, Institute for Advanced Studies in Basic Sciences, Zanjan, Iran, n.ajorlou@iasbs.ac.ir*

[3] *Professor, Department of Earth Sciences, Institute for Advanced Studies in Basic Sciences, Zanjan, Iran, aghods@iasbs.ac.ir*

[4] *Assistant Professor, Université Grenoble Alpes, ISTerre, Grenoble, France, james.hollingsworth@univ-grenoble-alpes.fr*

ABSTRACT

Landslides triggered by earthquakes are very important in earthquake risk assessment. To have a better understanding of their relation with characteristics of earthquakes and geomorphologic/geologic features of an area, the first step is to document size and geographic distribution of the landslides. The 20 June 1990 Rudbar earthquake (M_w 7.3) occurred in a mountainous area and is very well known for its destructive landslides. There is not yet a detail study on mapping of all the Rudbar earthquake induced landslides. In this research, we study distribution of these landslides within the isoseismal area with a MMI larger or equal than eight. We use Optical Image Correlation derived deformation maps, Google Earth imagery, as well as pre- and post-earthquake SPOT satellite images and aerial photos. All the used methods can detect fast-sliding earthquake-induced landslides. We have mapped 60 and 65 fast-sliding landslides by investigating Google Earth imagery/aerial photos and OIC displacement maps, respectively. The greatest fast-sliding landslides are concentrated around Baklor segment (~25-35 km distance west of the epicenter) and are dominantly due to re-sliding of the previous landslides. Some of the fast-sliding landslides created natural dams along their nearby stream channels. Slow-sliding landslides, with maximum displacement up to three meters, are only deduced from OIC deformation map.

Keywords: 20 June 1990 Rudbar earthquake, Earthquake-induced landslides, Optical Image Correlation, Remote-sensing.

INTRODUCTION

In the context of Earthquake-related hazards, coseismic landslides are one of the most important natural disasters that could cause serious damages to the infrastructures as well as financial and life losses. Therefore, there are lots of studies in recent decades focusing on relation between characteristics of earthquake-induced landslides with characteristics of earthquakes (e.g., Keefer, 1994, 1999 & 2002; Rodrigues et al., 1999; Khazai and Sitar, 2003; Malamud et al., 2004), and morphologic features of the epicenteral region (e.g., Meunier et al., 2008). Small magnitude earthquakes may results in landslides on susceptible slopes (Keefer, 1999) but larger magnitude ($M_L \geq 5.5$) earthquakes results in huge number of landslides mostly concentrated in areas with Modified Mercalli Intensity (MMI) of larger than five (Rodrigues et al., 1999; Keefer, 2002). The number of landslides is related with factors such as earthquake magnitude, focal depth, specific ground motion characteristics (vertical ground motion and horizontal peak ground motion) as well as distance from fault surface rupture and from epicenter (Keefer, 1994, 1999 & 2002; Rodrigues et al., 1999; Khazai and Sitar, 2003; Malamud et al., 2004). Also incoming S-waves and their direction with respect to the mountain range have strong effect on topography and location of landslides (Meunier et al., 2008). For an M_w 7 earthquake, studies reveal that landslides could be triggered to a maximum distance of ~200 km

from the epicenter (Keefer, 2002). To have a better insight about the characteristics of coseismic landslides, a wide documentation of landslides induced by earthquakes in wide variety of environments is needed (Keefer, 2002).

In Iran, the 20 June 1990 Rudbar earthquake (Fig. 1A) is well known for its earthquake-triggered landslides. The earthquake (M_w 7.3) occurred at depth of ~18 km along a WNW-striking sinistral fault plane. It results in ~80 km surface rupture composed of three right-stepping en-echelon segments, namely from east to west Zard-Goli, Kabateh and Baklor segments (Fig. 1A). Its triggered landslides causing serious damages to the roads and nearby villages and killed lots of people (Berberian et al., 1992). Due to rugged topography of the earthquake-stricken region, there is few studies on the characteristics of the Rudbar coseismic landslides (e.g., Zare, 1993; Shahrivar, 2006; Mahdavifar and Memarian, 2012; Khodashahi et al., 2017). Most of these researches are concentrated on landslides along the Sefid Rud river valley (Shahrivar, 2006; Mahdavifar and Memarian, 2012; Khodashahi et al., 2017). This motivates us to investigate surface distribution of Rudbar earthquake-induced landslides, which is a basic step in studying the characteristics of such landslides. To do this, we focus on using remote sensing methods including Optical Image Correlation (OIC) derived deformation maps, SPOT satellite images, aerial photos and Google Earth imagery.

METHODOLOGY

We study distribution of landslides triggered by Rudbar earthquake cluster by several remote sensing methods. We use Rudbar earthquake coseismic surface deformation map (Fig. 1B) deduced from OIC method (Ajorlou, et al., in preparation) to find earthquake-related landslides. The OIC east-west deformation maps, marked by gray polygons on Figure 1A, cover parts of the region with MMI of larger than eight. We also manually plot the landslides at the mesoseismal area of the 1990 Rudbar earthquake (Berberian et al., 1992) using Google Earth imagery. Then, by comparing the pre- and post-earthquake aerial photos (scale 1:20000 for 1968 and scale 1:40000 for 2001 and 2003) as well as pre- and post-earthquake satellite images (1989 and 1994 SPOT panchromatic 10 m), we discern those landslides which were triggered by Rudbar earthquake (Fig. 1A). To evaluate the results of OIC method, we compare its results against those from other methods (Fig. 1B).

CONCLUSION

We plot the Rudbar coseismic landslides (Fig. 1A and B), in the region with MMI of equal or larger than eight. Comparing the result of different remote sensing methods indicates that the triggered landslides mapped by Google earth and aerial photos (Fig. 1A) are the fast-sliding ones. They concentrate in an area with ~13 km wide around the Rudbar earthquake surface rupture. The majority of the fast-sliding landslides have occurred in areas affected by previous landslides (Fig. 1C). The largest landslides resulted in formation of natural dams along their nearby river channel occurred around Baklor segment (Fig. 1A), ~25-35 km west of the mainshock epicenter. The fast-sliding landslides are also detectable by their white color in the OIC east-west deformation maps due to the image decorrelation in these maps (Fig. 1B and C). We plot 60 and 65 fast-sliding landslides detected by Google earth imagery/aerial photos and OIC east-west deformation maps, respectively (Fig. 1A), within the regions with MMI larger than eight.

Slow-sliding triggered landslides have been only detected by the OIC method (Fig. 1B). Depending on the dip-direction of the surface topography, down-dip sliding of material in east-facing and west-facing slopes can be detected by positive and negative displacements, up to three meters, respectively (Fig. 1B).

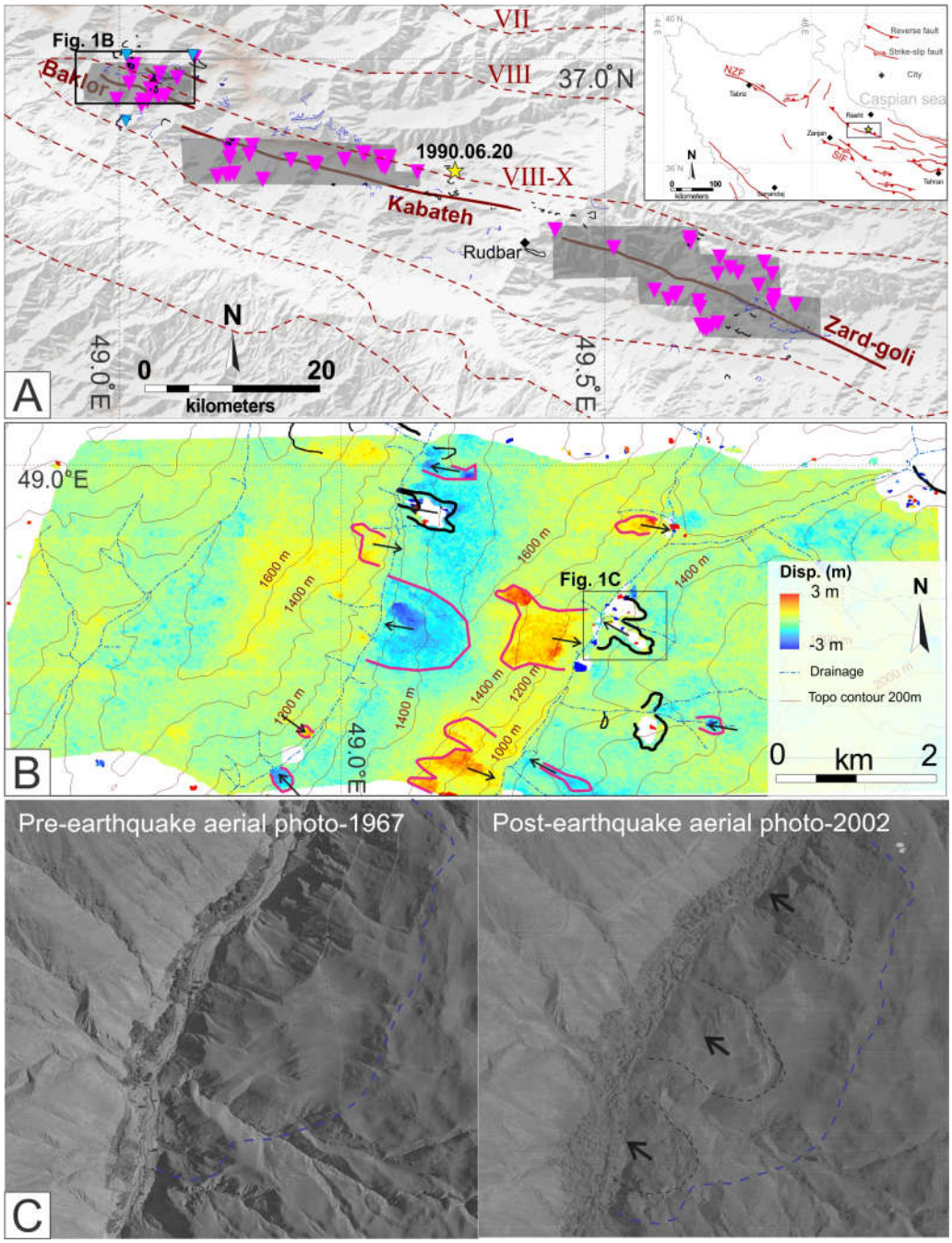

Figure 1. A) The inset map presents location of the study area. Faults in are from Hessami et al. (2003). The main figure includes old and coseismic triggered landslides (blue and black lines, respectively) induced from Google Earth imagery and aerial photos, Fast-sliding landslides deduced from OIC east-west deformation map (Pink rectangles) and coverage area of our aerial photos used in OIC method (grey transparent polygons). Blue rectangles are natural lakes due to the triggered landslides. Dashed red lines are Modified Mercalli Intensity (MMI) isoseimal regions. Bold red lines are Rudbar earthquake surface rupture from (Berberian et al., 1992). Yellow star is the epicenter of 20 June 1990 Rudbar mainshock from Jozi (2014). B) OIC east-west deformation map of Baklor segment (Ajorlou, et al., in preparation) presents distribution of Rudbar earthquake-induced landslides. Black lines are fast triggered landslides which are visible at aerial photos and satellite images and OIC deformation map. Red lines are slow triggered landslides defined only by OIC east-west deformation map. Black arrows show direction of sliding. C) Pre- and post- earthquake aerial photo reveal one of fast sliding triggered landslides. Black and blue dashed lines are fast earthquake-triggered and old landslides.

REFERENCES

-Ajorlou, N., Hollingsworth, J., Mousavi, Z., Ghods, A., Masoumi, Z., in preparation. Characterizing surface deformation in the 1990 Rudbar earthquake (Iran) using optical image processing.

-Berberian, M., Qorashi, M., Jackson, J.A., Priestley, K. and Wallace, T., 1992. The Rudbar-Tarom earthquake of 20 June 1990 in NW Persia: preliminary field and seismological observations, and its tectonic significance. Bulletin of the Seismological Society of America, 82(4), pp.1726-1755.

-Hessami et al. (2003).

-Jozi (2014

-Keefer, D.K., 1994. The importance of earthquake-induced landslides to long-term slope erosion and slope-failure hazards in seismically active regions. In Geomorphology and Natural Hazards (pp. 265-284). Elsevier.

-Keefer, D.K., 1999. Earthquake-induced landslides and their effects on alluvial fans. Journal of Sedimentary Research, 69(1), pp.84-104.

-Keefer, D.K., 2002. Investigating landslides caused by earthquakes–a historical review. Surveys in geophysics, 23(6), pp.473-510.

-Khazai, B. and Sitar, N., 2004. Evaluation of factors controlling earthquake-induced landslides caused by Chi-Chi earthquake and comparison with the Northridge and Loma Prieta events. Engineering geology, 71(1-2), pp.79-95.

-Khodashahi, M., Rahimi, E. and Bagheri, V., 2018. Earthquake-Induced Landslides Hazard Zonation of Rudbar-Manjil Using CAMEL Model. Geotechnical and Geological Engineering, 36(2), pp.1319-1340.

-Mahdavifar, M. and Memarian, P., 2013. Assessment of earthquake-induced landslides triggered by Roudbar-Manjil earthquake in Rostamabad (Iran) quadrangle using knowledge-based hazard analysis approach. In Earthquake-Induced Landslides (pp. 769-780). Springer, Berlin, Heidelberg.

-Malamud, B.D., Turcotte, D.L., Guzzetti, F. and Reichenbach, P., 2004. Landslides, earthquakes, and erosion. Earth and Planetary Science Letters, 229(1-2), pp.45-59.

-Meunier, P., Hovius, N. and Haines, J.A., 2008. Topographic site effects and the location of earthquake induced landslides. Earth and Planetary Science Letters, 275(3-4), pp.221-232.

-Rodrıguez, C.E., Bommer, J.J. and Chandler, R.J., 1999. Earthquake-induced landslides: 1980–1997. Soil Dynamics and Earthquake Engineering, 18(5), pp.325-346.

-Shahrivar, H., 2006. The morphology, setting and processes of Rudbar and Fatalak Landslides: triggered by the 1990 Manjil-Rudbar earthquake in Iran (Master's thesis).

-Zaré, M., 1993. Macrozonation of landslides for the Manjil, Iran 1990 earthquake.